

Enhancement of superconducting fluctuations in a correlated electron system coupled to the lattice

A. A. Zvyagin,^{1,2,3} V. V. Slavin,^{1,3} and G. A. Zvyagina¹

¹*B. I. Verkin Institute for Low Temperature Physics and Engineering of the National Academy of Sciences of Ukraine, Nauky Avenue 47, Kharkiv 61103, Ukraine*

²*Max-Planck Institut für Physik komplexer Systeme, Nöthnitzer Straße 38, D-01187 Dresden, Germany*

³*V. N. Karazin Kharkiv National University, 4 Svoboda Square, Kharkiv 61022, Ukraine*



(Received 4 May 2023; revised 3 July 2023; accepted 14 July 2023; published 31 July 2023)

Using the exact Bethe ansatz solution, a one-dimensional correlated electron system coupled to the lattice is considered. Electrons belonging to two orbital bands interact via the exchange coupling. It is shown that the coupling to the lattice strains can produce a phase transition to the state in which the degeneracy in the orbital filling is removed. In such a state the formation of superconducting correlations is enhanced. The influence of the external magnetic field on the transition is studied.

DOI: [10.1103/PhysRevB.108.045428](https://doi.org/10.1103/PhysRevB.108.045428)

I. INTRODUCTION

In recent years, physicists have investigated correlated electron systems with nonstandard ordering. One example of a system with nonconventional ordering is the so-called nematic electron system with rotational symmetry breaking. Systems with broken rotational symmetry are similar to ordered states of molecules in liquid crystals [1] where the distinguished orientation is present. However, unlike, e.g., the magnetization (the order parameter in magnetically ordered systems), a vector, which violates the time-reversal symmetry, the order parameter in nematic systems is a director [2], which violates the rotational O(3) symmetry. Nematic properties were observed in many correlated electron materials, such as rare-earth insulators [3], heavy-fermion systems [4], and iron-based superconductors [5–8]. Among other unconventional superconductors, iron-based strongly correlated electron systems manifest many interesting phenomena caused by the competition between different electronic interactions and their multiband structure [9]. Large intra-atomic exchange caused by the Hund interaction in those materials [10,11] yields a high level of orbital dependency of their properties [12]. For example, the excitation bands related to the d_{xz} and d_{yz} orbitals have metallic character, while the d_{xy} orbital is believed to be more insulating. Due to such a symmetry breaking, electronic properties can be influenced; see, e.g., studies of the orbital-dependent pairing [13] and angle-resolved photoemission spectra [14]. For instance, the iron-based material FeSe, due to a relatively high transition temperature, manifests properties that can be caused by the presence of nematic, maybe

magnetic, and superconducting orderings, such as orbitally dependent band shifts which can affect pair formation, a high level of electron-electron correlations, and electronic nematic behavior. It is important to stress that FeSe becomes superconducting at 9 K, at temperatures below the temperature of the phase transition to the orthorhombic lattice state (at 90 K) [15], at which, e.g., the d_{xz} and d_{yz} orbitals have to manifest different properties from the d_{xy} orbital. The origin of superconductivity, in particular of the pairing between electrons in iron-based superconductors, remains an open question. There exists a suggestion to use, for the explanation of pairing, spin and orbital nematic fluctuations [16,17], based on various experimental findings for iron-based superconducting materials. For example, some theories emphasize the role of the Hund interaction, i.e., the exchange interaction there [18,19].

For one-dimensional quantum correlated electron models, exact quantum mechanical solutions are known [20]. Integrability permits one to obtain theoretically their characteristics exactly. On the other hand, features of the one-dimensional density of states enhance quantum and thermal fluctuations there. Those fluctuations often destroy the long-range ordering for quantum systems with gapless excitations for nonzero temperatures [21]. However, in the ground state, some one-dimensional quantum systems with gapped excitations can manifest a long-range ordering [22,23], with quantum phase transitions between ordered and disordered phases. Also, for correlated electron systems with emerging gapless excitations, correlation functions decay with distance and time algebraically (this decay is slower than the exponential decay for systems with only gapped excitations), and therefore correlations between particles are very strong there.

Our study is motivated by effects of nematicity observed in iron-based superconducting materials, i.e., the breaking of the rotational symmetry. Due to the change in the symmetry, probably caused by orthorhombic lattice distortions, itinerant electron bands related to different orbitals can play an

Published by the American Physical Society under the terms of the Creative Commons Attribution 4.0 International license. Further distribution of this work must maintain attribution to the author(s) and the published article's title, journal citation, and DOI. Open access publication funded by the Max Planck Society.

important role in the onset of superconducting correlations. In this paper we study the effect of the lattice distortions on the electronic properties of the correlated electron system. For this purpose we use a one-dimensional model that is exactly solvable by the Bethe ansatz, in which both orbital and spin degrees of freedom of itinerant electrons which interact via the exchange (Hund-like) coupling are taken into account exactly. Naturally, a one-dimensional model cannot describe the behavior of iron-based superconducting materials. Nonetheless, we believe that some features of the pair formation and their stability—in particular, caused by the external magnetic field and the interaction with the lattice distortions, which can be obtained exactly in the framework of the considered model—can shed additional light on the nature of the superconductivity there. Most other theoretical methods, used for the description of such systems, are either perturbative, like the diagrammatic technique, or based on mean-field-like schemes or Ginzburg-Landau-like theories. In the latter the interaction between the nematicity and superconductivity can be considered only as the coupling between related order parameters and often cannot rely on the microscopic origin of those two effects. On the other hand, using our exact results, it will be more clear how to construct a Ginzburg-Landau-like

theory for a more realistic three-dimensional model, in which pair creation and pair stability follow from the mechanism of interaction between electrons belonging to bands formed by different orbitals. In our approach the nematicity is taken into account via the splitting of the itinerant electron bands: The anisotropy of the lattice induces different potentials (e.g., the action of the crystalline electric field) of ions affecting itinerant electrons. We study how the interaction of the one-dimensional correlated electrons with the lattice can strongly influence superconducting fluctuations of correlated electrons. We show that due to the electron-lattice coupling, orbital degeneracy (equal filling of orbital bands) is lifted and, as a result, the effective coupling between electrons in Cooper-like spin singlet pairs is enhanced. We also study the influence of the external magnetic field on the considered effect. The effects predicted in this paper can also be related to some valence skipping materials with antiferromagnetic exchange (Hund-like) couplings, such as fullerenes, etc.

II. EXACTLY SOLVABLE MODEL

Let us consider the one-dimensional correlated electron system which can be described by the Hamiltonian

$$\begin{aligned} \mathcal{H}_0 = & \sum_{m,\sigma} \int dx c_{m,\sigma}^\dagger(x) \left[\frac{\partial^2}{\partial x^2} \right] c_{m,\sigma} + c \sum_{m,m',\sigma,\sigma'} \int dx_1 \int dx_2 \delta(x_1 - x_2) c_{m,\sigma}^\dagger(x_1) c_{m',\sigma'}^\dagger(x_2) c_{m',\sigma}(x_2) c_{m,\sigma}(x_1) \\ & - \frac{H}{2} \sum_m \int dx [c_{m,\uparrow}^\dagger(x) c_{m,\uparrow}(x) - c_{m,\downarrow}^\dagger(x) c_{m,\downarrow}(x)] + D \sum_{m,\sigma} (-1)^m \int dx c_{m,\sigma}^\dagger(x) c_{m,\sigma}(x), \end{aligned} \quad (1)$$

where $c_{m,\sigma}^\dagger(x)$ [$c_{m,\sigma}(x)$] creates (destroys) the electron with the coordinate x ; spin $\sigma = \uparrow, \downarrow$, which belongs to the orbital band, enumerated by the index $m = 1, 2$; $c > 0$ is the exchange coupling constant; H is the external magnetic field; and D is the parameter which determines the splitting between orbital bands. Notice that nonzero D produces different chemical potentials $\mu \pm D$ (μ is the chemical potential) for electrons belonging to each orbital band. It is supposed that electrons in each orbital band have equal masses (equal to $1/2$). The interaction is of the exchange (Hund-like) type. Notice, however, that in atomic physics, Hund's exchange coupling yields the maximum spin value of the electrons filling the orbital. Similar behavior, in which Hund's exchange produces the maximal value of the total spin, is characteristic for the so-called Hund metals [24]. In our model, instead, the choice of the sign of the exchange constant c is such that it produces the minimum value of the spin of coupled electrons. In particular, it produces the formation of spin singlet pairs, characteristic for iron-based superconducting materials. On the other hand, the sign of the exchange constant, characteristic of the Hund's coupling, will produce spin triplet pairing [25], which has not been observed in iron-based superconducting materials, at least as of yet. For the derivation of the Hamiltonian \mathcal{H}_0 from general grounds, see Appendix A.

Within the considered model, electrons with the same orbital index (and with opposite spins) experience an attraction, while for electrons with equal spins but with different orbital indices the interaction is repulsive. The model is known to be integrable [26], as the particular case of the more general one-dimensional model of particles with two indices and the local exchange interaction. The model is reduced to the one of the integrable one-dimensional Fermi gas with the δ -function repulsion [27,28] in the spin-polarized magnetic field, in which electrons with only one spin projection play a role. On the other hand, the model is reduced to the one of the integrable one-dimensional Fermi gas with the δ -function attraction for the only one orbital band filled.

The details of the exact Bethe ansatz solution for the system described by the Hamiltonian \mathcal{H}_0 are presented in Appendix B.

III. THE GROUND STATE BEHAVIOR

We describe the ground state properties of the correlated electron model by studying the solution of coupled integral equations for so-called dressed energies [29]. The dressed energies are the energies of states, related to the densities (see Appendix B), “dressed” due to the electron-electron

interactions. These integral equations are

$$\begin{aligned}
 \varepsilon(k) &= k^2 - \mu - \frac{H}{2} + D - \int_{-Q}^Q d\lambda a_1(\lambda - k)\psi(\lambda) + \int_{-A_1}^{A_1} d\xi a_1(\xi - k)\kappa_1(\xi) + \int_{-A_2}^{A_2} d\xi a_2(\xi - k)\kappa_2(\xi), \\
 \psi(\lambda) &= 2\left[\lambda^2 - \frac{c^2}{4} - \mu + D\right] - \int_{-Q}^Q d\lambda' a_2(\lambda' - \lambda)\psi(\lambda') - \int_{-B}^B dka_1(k - \lambda)\varepsilon(k) + \int_{-A_1}^{A_1} d\xi a_2(\xi - \lambda)\kappa_1(\xi) \\
 &\quad + \int_{-A_2}^{A_2} d\xi [a_1(\xi - \lambda) + a_3(\xi - \lambda)]\kappa_2(\xi), \\
 \kappa_1(\xi) &= -2D + \int_{-Q}^Q d\lambda a_2(\lambda - \xi)\psi(\lambda) + \int_{-B}^B dka_1(k - \xi)\varepsilon(k) - \int_{-A_1}^{A_1} d\xi' a_2(\xi' - \xi)\kappa_1(\xi') - \int_{-A_2}^{A_2} d\xi' [a_1(\xi' - \xi) \\
 &\quad + a_3(\xi' - \xi)]\kappa_2(\xi'), \\
 \kappa_2(\xi) &= -4D + \int_{-B}^B dka_2(k - \xi)\varepsilon(k) + \int_{-Q}^Q d\lambda [a_1(\lambda - \xi) + a_3(\lambda - \xi)]\psi(\lambda) + \int_{A_1}^{A_1} d\xi' [a_1(\xi' - \xi) + a_3(\xi' - \xi)]\kappa_1(\xi') \\
 &\quad - \int_{-A_2}^{A_2} d\xi' [2a_2(\xi' - \xi) + a_4(\xi' - \xi)]\kappa_2(\xi'). \tag{2}
 \end{aligned}$$

Here, $\varepsilon(\pm B) = 0$, $\psi(\pm Q) = 0$, $\kappa_1(\pm A_1) = 0$, and $\kappa_2(\pm A_2) = 0$, i.e., $\pm B$, $\pm Q$, and $\pm A_{1,2}$ play the role of Fermi points for low-energy excitations.

Other eigenstates of the model are gapped. The ground state energy can be written as

$$\frac{E}{L} \equiv e_0 = \frac{1}{2\pi} \left[\int_{-B}^B dk \varepsilon(k) + 2 \int_{-Q}^Q d\lambda \psi(\lambda) \right]. \tag{3}$$

The ground state Bethe ansatz equations (2) and (B6) can be solved numerically by replacing the integrals by corresponding sums. The integral equations are transformed into systems of linear algebraic equations which can be solved numerically. In all calculations we set $c = 1$.

The obtained dependencies of magnetization per particle $m_z = M_z/N$ and the difference in the population of the bands per particle $l = \mathcal{L}/N$ as a function of applied magnetic field H at different values of chemical potential μ and band-splitting parameter D are presented in Figs. 1–4. Figures 2 and 3 demonstrate the dependencies M_z/N on H in the low-field limit. There one can see two critical values of the magnetic field in the $m_z(H)$ dependence. The lowest feature corresponds to the gap ($\Delta = 2H_c^{(1)}$) for unbound electron states. For $H < H_c^{(1)}$ the Fermi sea for unbound electron states is empty ($B = 0$). On the other hand, the high-field feature is related to the closing of the Fermi sea for Cooper-like spin singlet (and orbital triplet) pairs ($Q = 0$), which become gapped for $H > H_c^{(2)}$, where the spin-polarized phase takes place. At those critical values of the magnetic field, quantum phase transitions take place. The situation is reminiscent of the one for the type-II superconductors: For $H < H_c^{(1)}$ only Cooper-like spin singlet pairs play the main role in the low-energy properties, for $H > H_c^{(2)}$ only unbound electron states matter, and, finally, for $H_c^{(1)} < H < H_c^{(2)}$ the mixed state takes place. The difference compared with the usual superconductors is natural for one-dimensional systems: Only quantum phase transitions take place in the considered correlated electron model. The lowest critical value $H_c^{(1)}$ decreases with the increase in the band-splitting parameter D , while the field of the spin-flip

transition ($H_c^{(2)}$) increases with D . The critical values of the magnetic field $H_c^{(1,2)}$ exist even for the situation in which all electrons belong to one orbital band. However, for a nonzero difference in the population of the bands, additional quantum phase transitions (critical values of the magnetic field) take place. Also, the magnetic field dependence of the difference

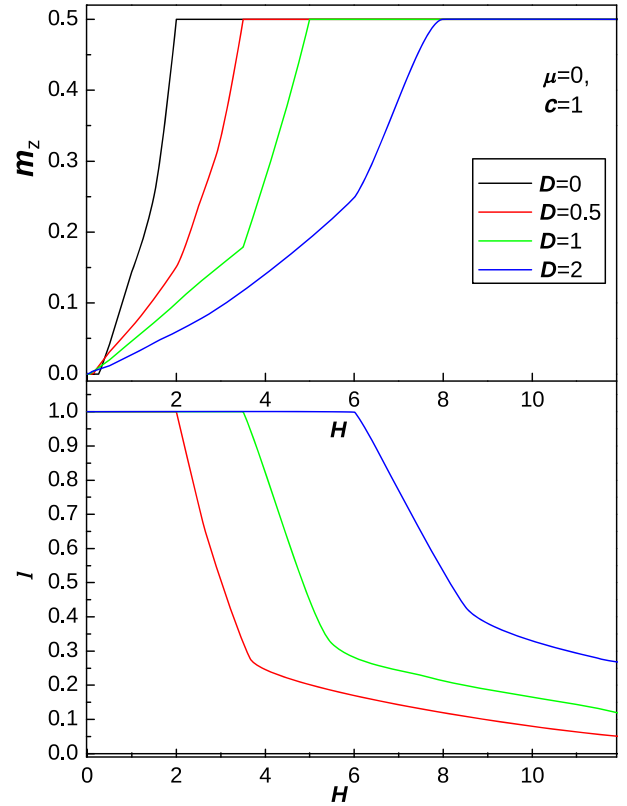


FIG. 1. The dependence of the projection of the magnetic moment per electron m_z and the difference in the population of the orbital bands per electron l on magnetic field H at $c = 1$ and $\mu = 0$.

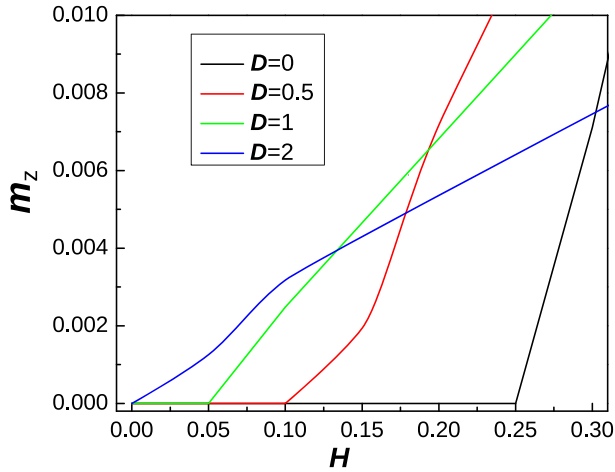


FIG. 2. $\mu = 0$. The dependence of m_z on H in the limit of small values of the magnetic field $H \ll 1$. One can see that the lower critical value of the magnetic field $H_c^{(1)}$ in the dependence decreases with the increase in orbital band-splitting parameter D .

in the population of orbital bands also manifests features at those quantum critical points, at which A_1 and A_2 become zero: At those quantum phase transitions the Fermi seas for orbital strings with $m = 1, 2$ become empty.

The increase in the chemical potential does not change qualitatively the ground state behavior of the projection of the magnetic moment and the difference in the population of the orbital bands. The values of the magnetic field at which

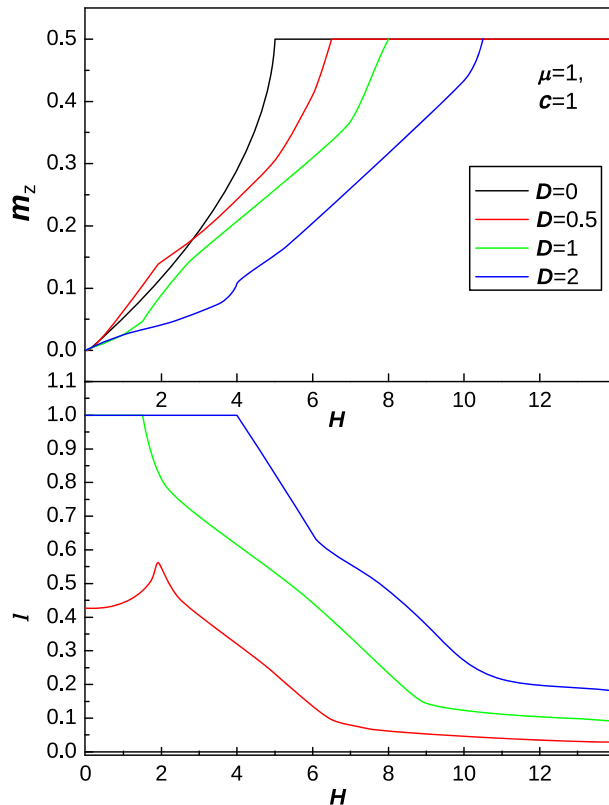


FIG. 3. The same as in Fig. 1, but for $\mu = 1$.

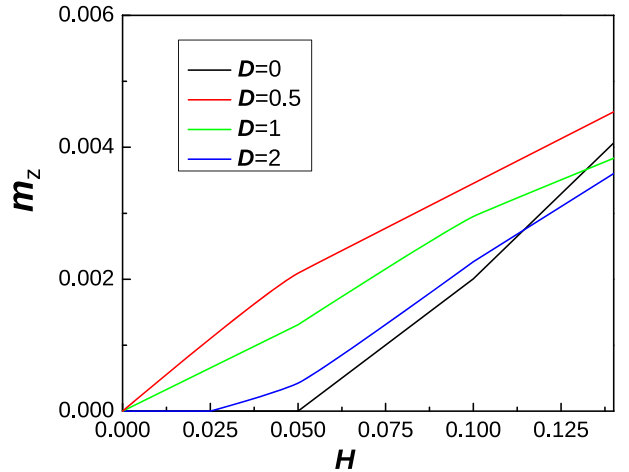


FIG. 4. The same as in Fig. 2, but for $\mu = 1$.

quantum phase transitions take place are renormalized due to the change in μ .

The dependencies of the lower ($H_c^{(1)}$) and upper ($H_c^{(2)}$) critical values of the magnetic field on the splitting parameter D for $\mu = 0$ and $\mu = 1$ are presented in Figs. 5 and 6.

We have also calculated the dependencies of critical values of splitting parameters $D_c^{(1)}$ and $D_c^{(2)}$ on the magnetic field H (see Fig. 7). These critical values correspond to the vanishing of interorbital band states, i.e., to the Fermi points for κ_1 and κ_2 [see (2)]. Notice that the dependencies of $D_c^{(1)}$ and $D_c^{(2)}$ on N at $H = 0$ were obtained in Ref. [29]. Our results are in a good agreement with those data. At the critical lines of quantum phase transitions the ground state magnetic and orbital susceptibilities manifest square-root singularity, $\chi \sim |H - H_c|^{-1/2}$ and $\chi_L \sim |D - D_c|^{-1/2}$; at the tricritical points of crossing of two critical lines the singularity exponents become $-3/4$.

Of special interest are the magnetic field and splitting parameter dependencies of the difference in the population of the orbital bands $l = \mathcal{L}/N$ (lower panels of Figs. 1 and 3). If

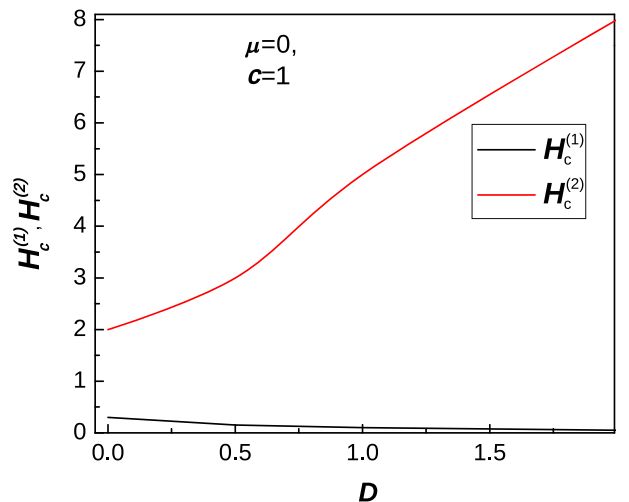
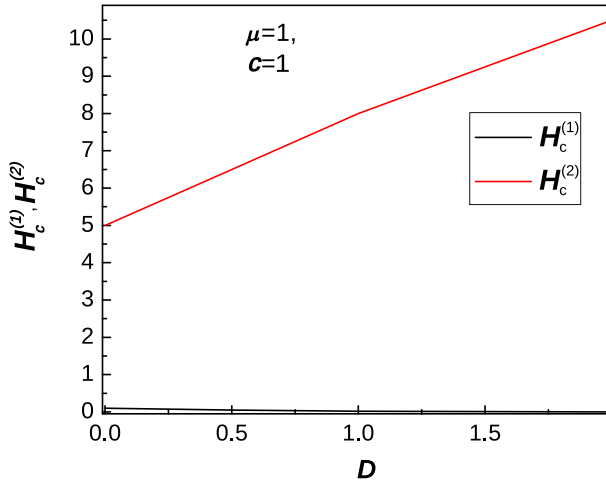
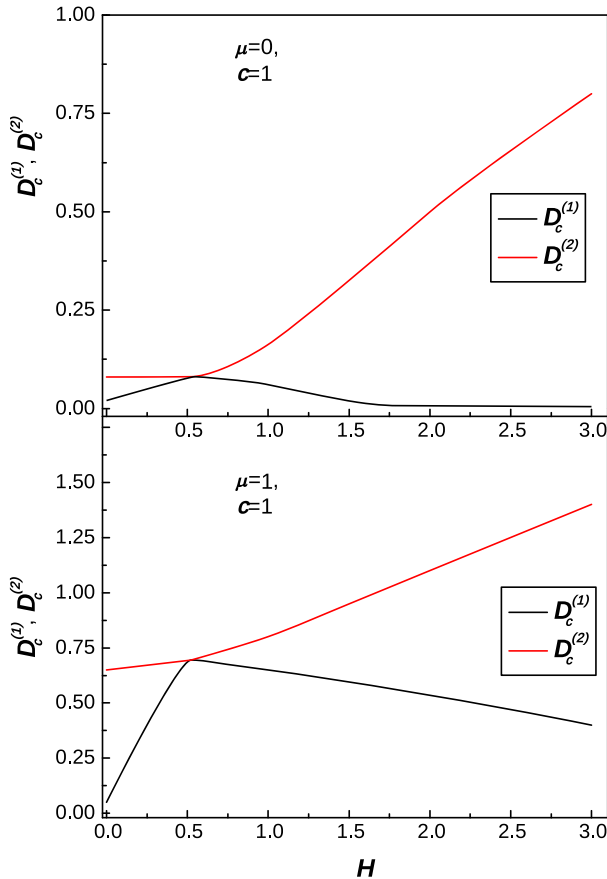
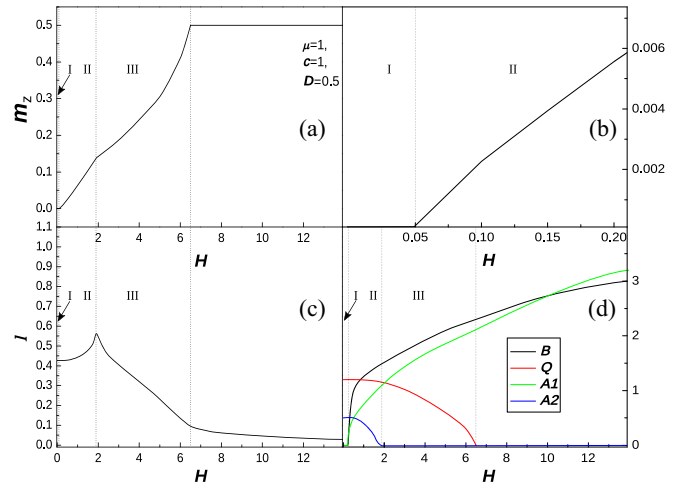


FIG. 5. The dependencies of the critical values of the magnetic field $H_c^{(1)}$ and $H_c^{(2)}$ on the band splitting parameter D for $\mu = 0$.


 FIG. 6. The same as in Fig. 5, but for $\mu = 1$.

$D < D_c^{(1)}$, then $l = 0$ for all values of the magnetic field H , which corresponds to the equal filling of the orbital bands. If $D_c^{(1)} \leq D \leq D_c^{(2)}$, then $l < 1$ for all $H \geq 0$. For example, according to Fig. 6 for $\mu = 1$ we have $D_c^{(1)} \approx 0.01$ and $D_c^{(2)} \approx 0.65$, and as seen from Fig. 3, for $D = 0.5$ (red curve) the difference in the population of the orbital bands $l < 1$ for


 FIG. 7. The dependencies of the critical values of the orbital band-splitting parameter $D_c^{(1)}$ and $D_c^{(2)}$ on the magnetic field H at different values of the chemical potential μ .

 FIG. 8. The dependencies of (a) and (b) m_z , (c) l , and (d) B , Q , A_1 , and A_2 on the magnetic field H at $\mu = 1$ and $D = 0.5$.

all the values of the magnetic field H . This means that both orbital bands are filled partially (i.e., $\mathcal{M} < N/2$). It should be noted that just this partial orbital band filling provides a gain in total energy (3). Otherwise, if $D > D_c^{(2)}$, there exists a range of values of the magnetic field H where all electrons occupy only one band, $\mathcal{M} = 0$ and, hence, $l = 1$. Then, with an increase in the magnetic field H a part of the electrons passes into another orbital band in the limit $H \rightarrow \infty$, and we have again half-filling occupation of the bands (i.e., $l = 0$).

The analysis of $m_z(H)$ dependencies shows that all the peculiarities in these curves are related to the appearance or vanishing of occupied states in the corresponding Fermi seas. In other words, the corresponding Fermi points B , Q , A_1 , and A_2 manifest themselves. This means that $m_z(H)$ dependencies can demonstrate up to four peculiarities related to quantum phase transitions. For example, the dependence of m_z on H corresponding to $\mu = 1$ and $D = 0.5$ is presented in Fig. 8(a) (this curve is the same as the red curve in Fig. 3). As one can see, there is a gap in the dependence in the range $0 \leq H \leq H_c^{(1)} \approx 0.05$ [see Fig. 8(b)]. This range is marked as range I in the figure and is associated with the absence of the Fermi sea for unbound electron states. Hence, in range I, the parameter $B = 0$ [see Fig. 8(d), black curve]. Besides, as seen from Fig. 8(d), the Fermi sea corresponding to κ_1 has vanished, and $A_1 = 0$ (green curve). In range II the Fermi sea for unbound electron states appears, and thus $B > 0$. At $H \approx 1.9$, one can see a peculiarity in $m_z = M_z/N$ and $l = \mathcal{L}/N$ dependencies [see Figs. 8(b) and 8(c)], which correspond to the vanishing Fermi sea corresponding to κ_2 (i.e., $A_2 = 0$). In range II the number of unbound electron states increases (black curve), and the number of Cooper-like spin singlet pairs decreases (red curve). At $H = H_c^{(2)} \approx 6.5$ the Fermi sea for Cooper-like spin singlet pairs vanishes, and therefore $Q = 0$ (red curve).

IV. COUPLING TO THE LATTICE: PHASE TRANSITION

As we discussed above, the ions in the lattice produce different potentials (e.g., via the crystalline electric field) for itinerant electrons filling bands with different orbital indices. Let us consider a coupled electron-lattice system whose

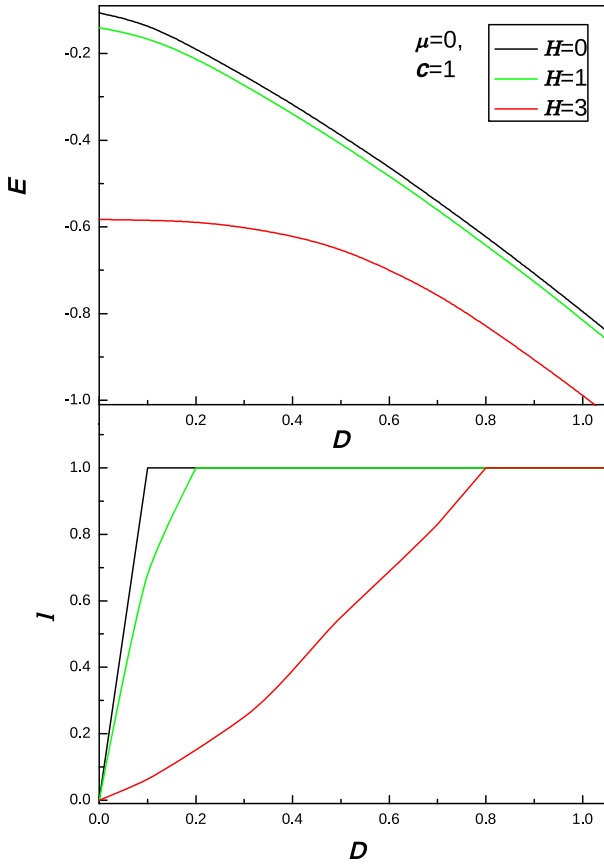


FIG. 9. The dependence of energy e_0 and difference in the population per particle l on the band-splitting parameter D for $\mu = 0$, $c = 1$, and $H = 0, 1, 3$.

Hamiltonian can be written as

$$\mathcal{H} = \mathcal{H}_0 + L \frac{C\epsilon^2}{2}, \quad (4)$$

where C is the elastic modulus, related to the strain ϵ , and $D = a\epsilon$, where a is the electron-lattice coupling constant. For example, the strain $\epsilon_{xx} - \epsilon_{yy}$ (and associated elastic modulus C_{66}) can be related to the phase transition from the tetragonal to the orthorhombic phase, as in FeS, or other iron-based superconductors. Such a strain induces the difference in the filling of, e.g., d_{xz} and d_{yz} orbital bands with the metallic character of the behavior. Such a difference is the manifestation of the orbital nematicity, i.e., the anisotropic behavior of the characteristics of the system.

We can show that a nonzero value of D yields a decrease in the energy of the correlated electron subsystem; see Figs. 9 and 10.

On the other hand, a nonzero value of ϵ produces an increase in the energy of the elastic subsystem. This is why a gain in the energy of the electron subsystem is compensated by a loss in the energy of the elastic subsystem. In other words, a phase transition between the states with zero and nonzero ϵ (zero or nonzero D) can take place. This phase transition is of the Jahn-Teller type: The degeneracy in filling of orbital bands is lifted due to nonzero D , caused by the lattice strain.

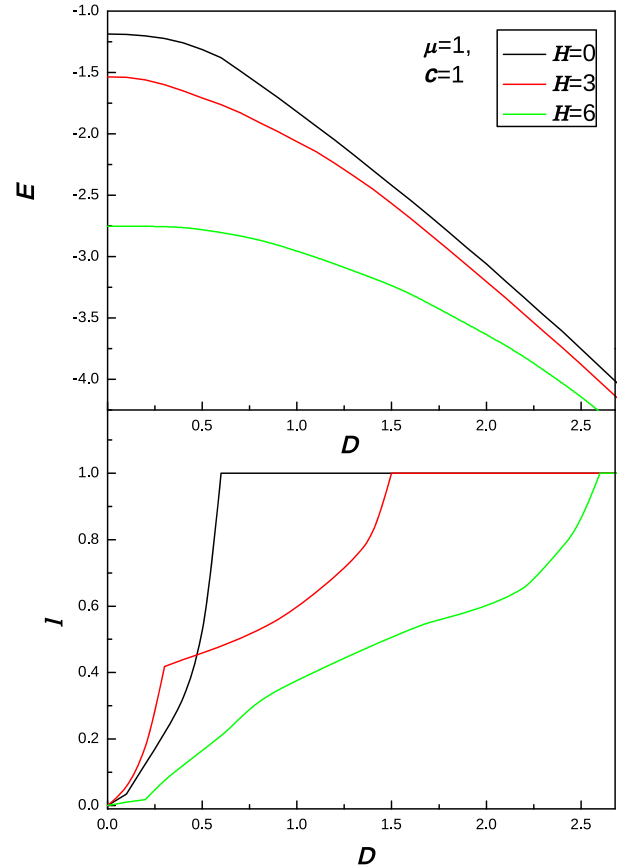


FIG. 10. The same as in Fig. 9, but for $\mu = 1$ and $H = 0, 3, 6$.

Obviously, at the phase transition we have

$$\frac{CD}{a^2} = \frac{\partial e_0}{\partial D}. \quad (5)$$

We can define the parameter $\alpha = C/a^2$, which measures the strength of the influence of the lattice on itinerant electrons. For weak electron-lattice coupling, α is large, while it is small for strong electron-lattice interaction. Graphical illustrations of Eq. (5) are presented in Figs. 11 and 12, in which solutions are presented for the cases of (i) zero magnetic field, (ii) intermediate magnetic field $H_c^{(1)} < H < H_c^{(2)}$, and (iii) strong magnetic field $H > H_c^{(2)}$ for two values of the chemical potential.

Notice that both $H_c^{(1)}$ and $H_c^{(2)}$ depend on D (see Figs. 5 and 6). According to Figs. 11 and 12, the condition of “intermediate values of the magnetic field” ($H_c^{(1)} < H < H_c^{(2)}$) is fulfilled in the total range of D if H is such that $H_c^{(1)}(D=0) < H < H_c^{(2)}(D=0)$. At the same time, the condition $H > H_c^{(2)}$ cannot be fulfilled in the region of D where l changes from 0 to 1 (see Figs. 5, 11, and 12). So, by the term “strong magnetic field” we mean the region in which the condition $H > H_c^{(2)}(D=0)$ is realized. The same situation takes place for the “weak magnetic field” region. We mean by this term the region in which $H < H_c^{(1)}(D=0)$ takes place.

We can see the following. For zero magnetic field (and, naturally for the region of weak magnetic fields) there are only two possibilities. Namely, for $\alpha > \alpha_c^{(1)} = 1.54$ the degeneracy between orbital bands is not lifted, and $l = \mathcal{L}/N = 0$

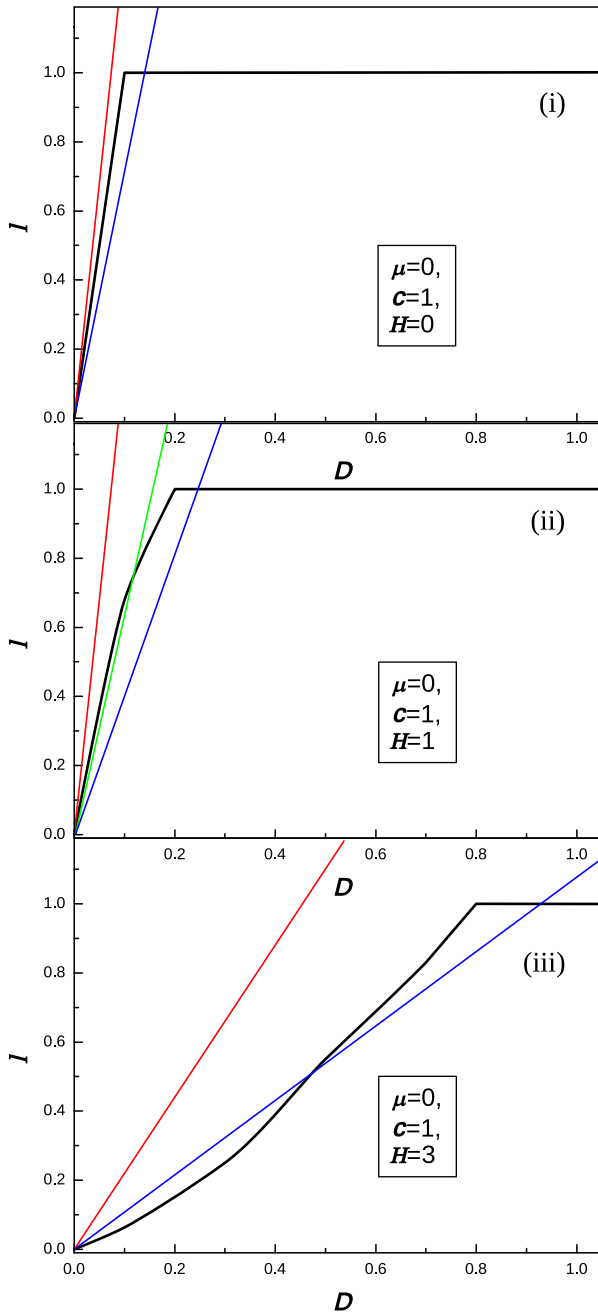


FIG. 11. Graphical solutions of Eq. (5) for $c = 1$, $H = 0, 1, 3$, and $\mu = 0$: case (i), zero magnetic field; case (ii), intermediate magnetic field; case (iii), strong magnetic field.

(weak connection between electron and lattice subsystems; red line). For $\alpha < \alpha_c^{(1)}$ the degeneracy is totally lifted, and $l = 1$ (strong coupling between electron and lattice subsystems; blue line).

For intermediate values of the magnetic field, three possibilities exist. First, for the weak coupling between electron and lattice subsystems $\alpha > \alpha_c^{(1)} = 1.26$ the degeneracy between orbital bands is not lifted (red line). For the intermediate coupling $\alpha_c^{(1)} > \alpha > \alpha_c^{(2)} = 1.11$ the degeneracy is partly lifted, and $0 < l < 1$ (green line). For the strong coupling $\alpha < \alpha_c^{(2)}$ the degeneracy between orbital bands is totally lifted $l = 1$ (blue line).

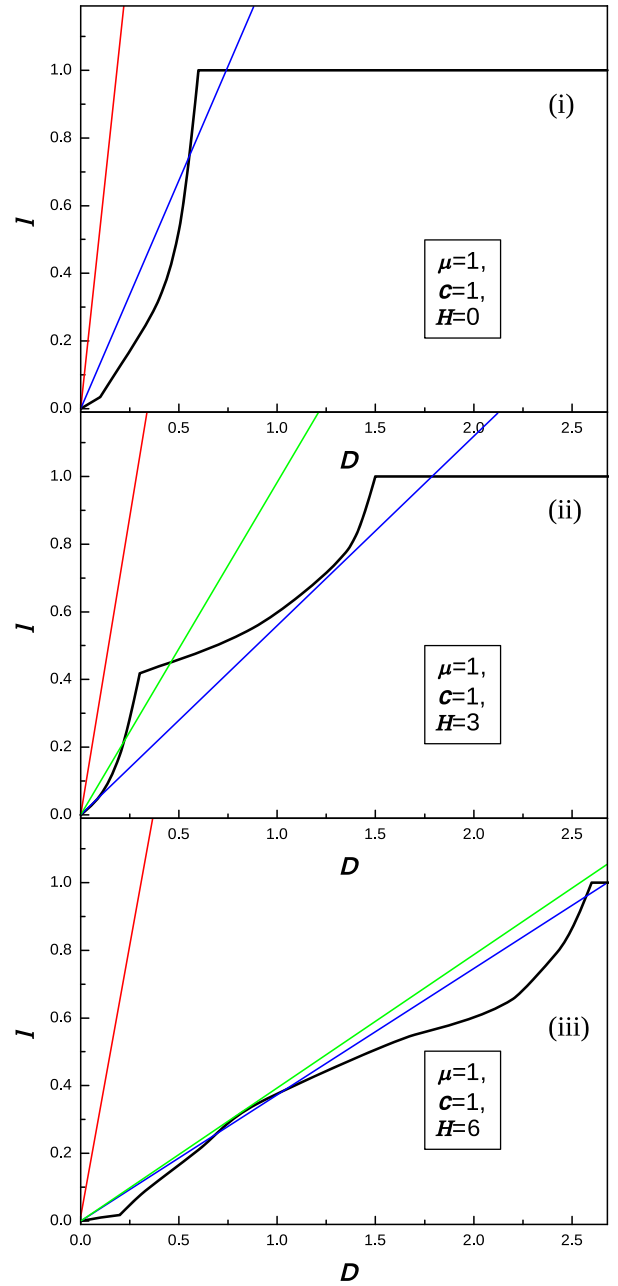


FIG. 12. The same as in Fig. 11, but for $\mu = 1$ and $H = 0, 3, 6$.

The case of a strong magnetic field ($H = 3$) is analogous to the small-field case. First, for the weak coupling between electron and lattice subsystems $\alpha > \alpha_c^{(1)} = 0.4$ the degeneracy between orbital bands is not lifted, and $l = 0$ (red line). For the strong coupling $\alpha < \alpha_c^{(2)} = 0.38$ the degeneracy between orbital bands is partly lifted, and $0 < l < 1$ (blue line). For strong magnetic fields the solutions related to the total lifting of the degeneracy are not realized.

The situation for $\mu = 1$ is similar to the case $\mu = 0$ for small and intermediate values of the magnetic field, except that critical values of the parameter α are renormalized. The qualitative difference from the case $\mu = 0$ described above appears only for large fields $H = 6$, for which the situation is reminiscent of the intermediate-field case. For weak coupling

between the electron subsystem and the lattice subsystem, one has $l = 0$ (red line), and orbital bands are degenerate. For strong coupling the degeneracy of the orbital bands is totally lifted, and $l = 1$ (blue line). For intermediate values of the parameter α the degeneracy of the orbital bands is partly lifted, so that $0 < l < 1$ (green line). Again, similar to the case $\mu = 0$, the solutions related to the total lifting of the degeneracy for strong magnetic fields are not realized.

Hence, due to the coupling between the correlated electron subsystem and the lattice, the strains in the latter cause the phase transition from the state with equal populations of the orbital bands to the states with partial populations, and with one orbital band depopulated. This phase transition is related to the onset of the nonzero value of the parameter D , proportional to the strain of the lattice, e.g., via the crystalline electric field, which regulates the relative population of the orbital bands. We can see how that phase transition changes the “superconducting” properties of the considered system. For example, for weak magnetic fields only Cooper-like spin singlet pairs exist. For the state with zero \mathcal{L} those states behave as free (noninteracting) particles with the critical exponent for the correlation function (it decays as $x^{-\gamma}$) $\gamma = 1$ [29]. On the other hand, if due to the nonzero strain the correlated electron subsystem is in the state with all electrons filling one orbital band, then the Hund-like interaction between electrons (the effective attraction between electrons with different spin) yields a decrease in the value of the critical exponent to the value $1/2 \leq \gamma \leq 1$, depending on the band filling (for the calculation of the asymptote of low-energy correlation functions of the considered correlated electron model, see, e.g., Ref. [30]). For the intermediate magnetic field case the calculation of the exponent is more complicated. For instance, at large values of c , one can write $\gamma = 1 - N(1 - 2m_z)/2L|c| \leq 1$. This means that superconducting correlations decay more slowly for the totally filled orbital band than for the case of the degenerate orbital band filling. It is important to point out that the features of the considered system in the domain $H_c^{(1)} < H < H_c^{(2)}$ can be related to the behavior of Hund’s impurity systems studied recently [31,32], according to which an intermediate spin-orbital selective phase may occur as a function of the temperature (and possibly as a function of external magnetic field at zero temperature). In that intermediate magnetic field domain, orbital degrees of freedom are quenched (in our approach due to the coupling to the lattice), but the spin still fluctuates. Hence the influence of the lattice enhances the effective attraction between electrons and the formation of the Cooper-like spin singlet pairs for correlated electrons with the exchange coupling. On the other hand, the nonzero value of D decreases the value of $H_c^{(1)}$, and increases the value of $H_c^{(2)}$, enlarging the range of magnetic fields in which superconducting correlations take place.

V. SUMMARY

In summary, motivated by observations in iron-based superconductors which reveal the nematicity of electron characteristics perhaps related to the lattice symmetry, we have studied a system which consists of a one-dimensional subsystem of correlated electrons and the lattice. The correlation between itinerant electrons filling two orbital bands is

supposed to be of the exchange type. The model for correlated electrons is integrable. Using the exact quantum mechanical solution, we have considered the interaction between the strains of the lattice and correlated electrons. We predict that such an interaction yields the Jahn-Teller-like phase transition, in which strains lift the orbital degeneracy of correlated electron bands. Due to the phase transition the itinerant electrons fill one of the orbital bands, while the other becomes empty. As a result, the formation of the superconducting correlations is enhanced, and the diapason of the values of the magnetic field, in which Cooper-like singlet pairs can exist, becomes larger. Naturally, the considered one-dimensional model cannot be directly applied to the description of iron-based superconductors. However, we believe that a similar mechanism can be applicable for more realistic models (which, on the other hand, do not permit exact quantum mechanical solutions).

ACKNOWLEDGMENTS

A.A.Z. thanks N. Konik for helpful discussions. V.V.S. and G.A.Z. acknowledge the support from the Pauli Ukraine Project, funded within the Wolfgang Pauli Institut Thematic Program “Mathematics-Magnetism-Materials.” G.A.Z. also acknowledges the financial support by the STCU, project “Magnetism in Ukraine Initiative,” Project Agreement No. 9918.

APPENDIX A

In this Appendix we show the origin of the considered Hamiltonian.

It is standard to consider ions of solids forming a static lattice. In this approach, one can write the approximate form of the general Hamiltonian of itinerant electrons in a crystal as [33–35]

$$\mathcal{H}_G = \sum_j \left[\frac{\mathbf{p}_j^2}{2m_e} + V(\mathbf{x}_j) \right] + \sum_{i,j} U(\mathbf{x}_i - \mathbf{x}_j), \quad (\text{A1})$$

where \mathbf{x}_j is the coordinate of the j th electron, \mathbf{p}_j is its momentum, m_e is the mass of the electron, $V(\mathbf{x}_j)$ is the periodic potential of ions, and $U(\mathbf{x}_i - \mathbf{x}_j)$ is the screened Coulomb interaction between the electrons. Let us denote the first term in \mathcal{H}_G as \mathcal{H}_{G0} . It is obviously the one-electron part of the Hamiltonian. The eigenfunctions of \mathcal{H}_{G0} are Bloch functions $\varphi_{m\mathbf{k}}(\mathbf{x}) = \exp(i\mathbf{k}\mathbf{x})u_{m\mathbf{k}}(\mathbf{x})$, where m is the band number, \mathbf{k} is the quasimomentum running over the first Brillouin zone, and $u_{m\mathbf{k}}(\mathbf{x})$ is the periodic function.

On the other hand, one can use the other basic eigenfunctions for the Hamiltonian \mathcal{H}_{G0} , namely, the Wannier functions $\phi_m(\mathbf{x} - \mathbf{R}_j)$, where \mathbf{R}_j denotes the position of the j th ion. The Bloch functions can be written as the Fourier transforms of the Wannier functions $\varphi_{m\mathbf{k}}(\mathbf{x}) = L^{-1/2} \sum_{\mathbf{R}_j} \exp(i\mathbf{k}\mathbf{R}_j)\phi_m(\mathbf{x} - \mathbf{R}_j)$, where L is the number of lattice sites.

Introduction of the operators $a_{m\mathbf{k},\sigma}^\dagger$ ($a_{m\mathbf{k},\sigma}$), which create (destroy) the electron in the Bloch state $\varphi_{m\mathbf{k}}(\mathbf{x})$ in the m th band with the spin $\sigma = \uparrow, \downarrow$ and the quasimomentum \mathbf{k} , and their Fourier transforms $a_{mj,\sigma}^\dagger$ ($a_{mj,\sigma}$) permits us to rewrite the

Hamiltonian \mathcal{H}_G in the second quantized form as

$$\mathcal{H}_G = \sum_{j,j',m,\sigma} t_{mj} (a_{mi,\sigma}^\dagger a_{mj,\sigma} + \text{H.c.}) + \frac{1}{2} \times \sum_{i,j,r,q} \sum_{m,m',l,l',\sigma,\sigma'} U_{ijrq}^{mm'l'l'} a_{mi,\sigma}^\dagger a_{m'j,\sigma'}^\dagger a_{lr,\sigma'} a_{l'q,\sigma}, \quad (\text{A2})$$

where

$$t_{mj} = \int d^3x \phi_m^*(\mathbf{x} - \mathbf{R}_i) \left[\frac{\mathbf{p}^2}{2m_e} + V(\mathbf{x}) \right] \phi_m(\mathbf{x} - \mathbf{R}_j) \quad (\text{A3})$$

are the hopping elements, and the overlap integrals $U_{ijrq}^{mm'l'l'}$ can be written as

$$U_{ijrq}^{mm'l'l'} = \int d^3x \int d^3y \phi_m^*(\mathbf{x} - \mathbf{R}_i) \phi_{m'}^*(\mathbf{y} - \mathbf{R}_j) \times U(\mathbf{x} - \mathbf{y}) \phi_l(\mathbf{x} - \mathbf{R}_r) \phi_{l'}(\mathbf{y} - \mathbf{R}_q). \quad (\text{A4})$$

Notice that some of the overlap integrals are zero due to symmetry reasons. It is commonly accepted to use the definitions for some overlap integrals such as $U = U_{ijij}^{mmmm}$, $U' = U_{ijij}^{mm'mm'}$, and $J = U_{ii,kk}^{mmmm'}$, which are known as the intraband and interband Coulomb and exchange constants, respectively.

One can take into account possible nonzero overlap (similar to the known approach for the hydrogen molecule [36,37]) of Bloch functions in different bands $Y = \int d^3x \phi_m^*(\mathbf{x}) \phi_{m'}(\mathbf{x})$. This yields the renormalization of the overlap integrals $\tilde{U}^{mm'l'l'}$ as

$$\begin{aligned} \tilde{U}_{ijij}^{mm'mm'} &= U_{ijij}^{mm'mm'} - \int d^3x U(\mathbf{x} - \mathbf{R}_i) |\phi_m(\mathbf{x})|^2 \\ &\quad - \int d^3x U(\mathbf{x} - \mathbf{R}_j) |\phi_{m'}(\mathbf{x})|^2, \\ \tilde{U}_{ijij}^{mm'm'm} &= U_{ijij}^{mm'm'm} - Y \int d^3x U(\mathbf{x} - \mathbf{R}_i) \phi_m^*(\mathbf{x}) \phi_{m'}(\mathbf{x}) \\ &\quad - Y \int d^3x U(\mathbf{x} - \mathbf{R}_j) \phi_{m'}^*(\mathbf{x}) \phi_m(\mathbf{x}), \end{aligned} \quad (\text{A5})$$

for the Hubbard and exchange interband integrals, respectively. In particular, the nonzero overlap of the interband Bloch functions can produce not only positive but also negative values of some renormalized overlap integrals.

It is possible to define the operators

$$\begin{aligned} c_{m,\sigma}^\dagger(\mathbf{x}) &= \sum_{\mathbf{k}} \phi_{m\mathbf{k}}^*(\mathbf{x}) a_{m\mathbf{k},\sigma}^\dagger = \sum_j \phi_m^*(\mathbf{x} - \mathbf{R}_j) a_{mj,\sigma}^\dagger, \\ c_{m,\sigma}(\mathbf{x}) &= \sum_{\mathbf{k}} \phi_{m\mathbf{k}}(\mathbf{x}) a_{m\mathbf{k},\sigma} = \sum_j \phi_m(\mathbf{x} - \mathbf{R}_j) a_{mj,\sigma}. \end{aligned} \quad (\text{A6})$$

Due to the space homogeneity, one can rewrite the overlap integral $\tilde{U}_{ijij}^{mm'l'l'} = \tilde{U}^{mm'l'l'}(\mathbf{x}_i, \mathbf{y}_j)$ as $\tilde{U}^{mm'l'l'}(\mathbf{x} - \mathbf{y})$, and using these creation and destruction operators, we can rewrite the Hamiltonian as

$$\begin{aligned} \mathcal{H}_G &= \sum_{m,\sigma} \int d^3x c_{m,\sigma}^\dagger(\mathbf{x}) \left[\frac{\mathbf{p}^2}{2m_e} + V(\mathbf{x}) \right] c_{m,\sigma}(\mathbf{x}) \\ &\quad + \frac{1}{2} \sum_{m,m',l,l',\sigma,\sigma'} \int d^3x \int d^3y c_{m,\sigma}^\dagger(\mathbf{x}) c_{m',\sigma'}^\dagger(\mathbf{y}) \\ &\quad \times \tilde{U}^{mm'l'l'}(\mathbf{x} - \mathbf{y}) c_{l,\sigma'}(\mathbf{y}) c_{l',\sigma}(\mathbf{x}). \end{aligned} \quad (\text{A7})$$

For instance, for the case of a single band and only intrasite electron-electron interactions (with the assumption that intersite interactions are small) it is possible to write the Hamiltonian as

$$\mathcal{H}_H = \sum_{i,j,\sigma} t_{ij} (a_{i,\sigma}^\dagger a_{j,\sigma} + \text{H.c.}) + \frac{U}{2} \sum_{i,\sigma\sigma'} a_{i,\sigma}^\dagger a_{i,\sigma'}^\dagger a_{i,\sigma'} a_{i,\sigma}, \quad (\text{A8})$$

in which the intrasite Coulomb integral is defined as U . Such a Hamiltonian is known as the Hubbard Hamiltonian [38]. For the one-dimensional situation with nonzero hopping elements for the nearest-neighbor sites it is reduced to the exactly solvable model [39]

$$\mathcal{H}_H = -t \sum_{j,\sigma} (a_{j,\sigma}^\dagger a_{j+1,\sigma} + \text{H.c.}) + U \sum_j n_{j,\uparrow} n_{j,\downarrow}, \quad (\text{A9})$$

where $n_{j,\sigma} = a_{j,\sigma}^\dagger a_{j,\sigma}$.

In the continuum limit (see, e.g., Ref. [40]) the one-dimensional multiband Hamiltonian with only intrasite electron-electron interactions (others are assumed to be small) can be written as

$$\begin{aligned} \mathcal{H}_G &\approx a^2 \sum_{m,\sigma} t_m \int dx c_{m,\sigma}^\dagger(x) \frac{\partial^2}{\partial x^2} c_{m,\sigma}(x) \\ &\quad + 2a \sum_{m,m',l,l',\sigma,\sigma'} \int dx \int dy \delta(x-y) c_{m,\sigma}^\dagger(x) c_{m',\sigma'}^\dagger(x) \\ &\quad \times \tilde{U}^{mm'l'l'}(x-y) c_{l,\sigma'}(y) c_{l',\sigma}(y), \end{aligned} \quad (\text{A10})$$

where a is the intersite distance. For a single band in the one-dimensional case it reduces to the Hamiltonian of the one-dimensional Fermi gas with the δ -function interaction, which permits the exact solution [27,28].

The Hamiltonian \mathcal{H}_0 of the main text is the special case of this Hamiltonian for two bands with the same hopping elements for each band and the nonzero renormalized interband exchange integral (other overlap integrals are assumed to be zero).

APPENDIX B

In this Appendix we show the features of the exact Bethe ansatz solution for the correlated electron system with the Hamiltonian \mathcal{H}_0 .

It was shown [26] that the two-particle scattering matrix has the form

$$\hat{S}(k) = \frac{k\hat{I}_\sigma - ic\hat{P}_\sigma}{k - ic} \frac{k\hat{I}_m + ic\hat{P}_m}{k + ic}, \quad (\text{B1})$$

where k is the difference between quasimomenta of two electrons, \hat{I}_σ is the unity matrix in the spin subspace, \hat{P}_σ is the permutation operator in the spin subspace, \hat{I}_m is the unity matrix in the orbital subspace, and \hat{P}_m is the permutation operator in the orbital subspace. Each factor is 1 when applied to

the triplet state (with maximal spin or orbital moment) in the spin or orbital subspace. Therefore the two-particle scattering matrix acts nontrivially on the singlet (with minimal spin or orbital moment) spin or orbital parts of the wave function of electrons. Obviously, the two-particle scattering matrix factorizes (i.e., it acts independently) in the spin and orbital subspace. The two-particle scattering matrix in each subspace satisfies the Yang-Baxter equation (see, e.g., Ref. [20]), and therefore the model is Bethe ansatz integrable.

Within the Bethe ansatz scheme each eigenstate of the system described by the Hamiltonian \mathcal{H}_0 is determined by the set of quantum numbers called rapidities. The charge rapidities (quasimomenta of electrons) $\{k_j\}_{j=1}^N$, with N being the number of electrons, describe the excitations with the charge transfer. The spin rapidities $\{\lambda_\alpha\}_{\alpha=1}^M$, with M being the number of electrons with spin \downarrow , describe the excitations, which change the spin of the system. Finally, the orbital rapidities $\{\xi_\beta\}_{\beta=1}^{\mathcal{M}}$, with \mathcal{M} being the number of electrons in the second orbital band (we use $0 \leq \mathcal{M} \leq N/2$; for other values of filling of orbital bands, one can interchange indices 1 and 2 and $D \rightarrow -D$), describe excitations with the change in the orbital moment. For the periodic boundary conditions in the ring of length L the rapidities satisfy the set of Bethe ansatz equations

$$\begin{aligned}
e^{ik_j L} &= \prod_{\alpha=1}^M X_{c/2}^{-1}(k_j - \lambda_\alpha) \prod_{\beta=1}^{\mathcal{M}} X_{c/2}(k_j - \xi_\beta), \\
j &= 1, \dots, N, \\
\prod_{j=1}^N X_{c/2}(\lambda_\alpha - k_j) &= - \prod_{q=1}^M X_c(\lambda_\alpha - \lambda_q), \\
\alpha &= 1, \dots, M, \\
\prod_{j=1}^N X_{c/2}(\xi_\beta - k_j) &= - \prod_{q=1}^{\mathcal{M}} X_c(\xi_\beta - \xi_q), \\
\beta &= 1, \dots, \mathcal{M},
\end{aligned} \tag{B2}$$

where

$$X_n(u) = \frac{u + in}{u - in}. \tag{B3}$$

Due to the Fermi-Dirac nature of wave functions all rapidities within a given set have to be different to guarantee the linear independence of eigenfunctions. The energy of the state, which is described by the set of rapidities, is equal to

$$E = \sum_j k_j^2 - HM_z - D\mathcal{L}. \tag{B4}$$

Here, the projection of the total spin is $M_z = (1/2)(N - 2M)$. On the other hand, the value $\mathcal{L} = N - 2\mathcal{M}$ is the difference in the population of two bands with different orbital indices. In fact, it determines the nematicity of the considered model, because it is caused by the anisotropy of the ion potentials in the crystal lattice.

If $M = 0$, the model reduces to the one of the integrable one-dimensional Fermi gas with δ -function repulsion [27,28]. If $\mathcal{M} = 0$, the model reduces to the one of the integrable one-dimensional Fermi gas with δ -function attraction.

As usual, one-dimensional quantum many-body systems reveal their most important behavioral features in the ground state. In Ref. [29] it was shown that the solutions to the set of Bethe ansatz equations can be classified as follows. First, there exist $N - 2\hat{M}$ solutions with real charge rapidities k_j , which describe unbound electron states. Second, there exist \hat{M} solutions with complex-conjugate pairs $k = \lambda \pm ic/2$, which describe spin singlet orbital triplet Cooper-like pairs. Then there exist M'_n string solutions of the length $n - 1$, $\lambda = \lambda'_n + ic(n + 1 - 2p)/2$ (with $p = 1, \dots, n$), which describe spin-transferring bound states. Finally, there exist m'_n string solutions of the length $n - 1$, $\xi = \xi'_n + ic(n + 1 - 2p)/2$ (with $p = 1, \dots, n$), which describe bound states of the transfers between orbital bands. Here, λ'_n and ξ'_n are real; they describe the transfer of the center of mass of the bound state. The imaginary part for bound states describes the relative movement (it is imaginary, which means that the wave function decays with the increase in the distance between excitations bound into the string). The number of solutions satisfies the following relations: $M - \hat{M} = \sum_{n=1}^{\infty} M'_n$ and $\mathcal{M} = \sum_{n=1}^{\infty} m'_n$. The ground state of the model is formed by the filling of Fermi seas (as usual for electrons), in which eigenstates with negative energies are totally filled and ones with positive energies are empty, for four states [29], namely, for unbound electrons, Cooper-like pairs, and orbital-transferring states with $n = 1, 2$.

In the thermodynamic limit, where $L, N, M, \mathcal{M} \rightarrow \infty$ with the ratios $N/L, M/L$, and \mathcal{M}/L being finite, one can replace the large set of Bethe ansatz equations by the small set of integral equations. Let us define $\varepsilon(k)$ as dressed energy of the unbound electron states with the density of rapidities $\rho(k)$, $\psi(\lambda)$ as dressed energy of the Cooper-like spin singlet orbital triplet pairs with the density of rapidities $\sigma(\lambda)$, and $\kappa_{n=1,2}(\xi)$ as dressed energies of the orbital string states with $n = 1, 2$, respectively (states related to the transfer between orbital bands and their bound states), with the densities of rapidities $\phi_{n=1,2}(\xi)$.

Let us denote

$$a_n(x) = \frac{1}{\pi} \frac{(nc/2)}{x^2 + (nc/2)^2}. \tag{B5}$$

The ground state integral equations, which describe densities of rapidities, are [29]

$$\begin{aligned}
\rho(k) &= \frac{1}{2\pi} - \int_{-Q}^Q d\lambda a_1(\lambda - k)\sigma(\lambda) \\
&\quad + \int_{-A_1}^{A_1} d\xi a_1(\xi - k)\phi_1(\xi) + \int_{-A_2}^{A_2} d\xi a_2(\xi - k)\phi_2(\xi), \\
\sigma(\lambda) &= \frac{1}{\pi} - \int_{-Q}^Q d\lambda' a_2(\lambda' - \lambda)\sigma(\lambda') \\
&\quad - \int_{-B}^B dka_1(k - \lambda)\rho(k) + \int_{-A_1}^{A_1} d\xi a_2(\xi - \lambda)\phi_1(\xi) \\
&\quad + \int_{-A_2}^{A_2} d\xi [a_1(\xi - \lambda) + a_3(\xi - \lambda)]\phi_2(\xi),
\end{aligned}$$

$$\begin{aligned}
\phi_1(\xi) &= \int_{-Q}^Q d\lambda a_2(\lambda - \xi)\sigma(\lambda) \\
&+ \int_{-B}^B dk a_1(k - \xi)\rho(k) - \int_{-A_1}^{A_1} d\xi' a_2(\xi' - \xi)\phi_1(\xi') \\
&- \int_{-A_2}^{A_2} d\xi' [a_1(\xi' - \xi) + a_3(\xi' - \xi)]\phi_2(\xi'), \\
\phi_2(\xi) &= \int_{-Q}^Q d\lambda [a_1(\lambda - \xi) + a_3(\lambda - \xi)]\sigma(\lambda) \\
&+ \int_{-B}^B dk a_2(k - \xi)\rho(k) \\
&- \int_{A_1}^{A_1} d\xi' [a_1(\xi' - \xi) + a_3(\xi' - \xi)]\phi_1(\xi') \\
&- \int_{-A_2}^{A_2} d\xi' [2a_2(\xi' - \xi) + a_4(\xi' - \xi)]\phi_2(\xi'). \quad (\text{B6})
\end{aligned}$$

The energy E , the number of electrons N , the magnetic moment M_z , and the difference in population between the first and the second orbitals \mathcal{L} per site (L is the number of sites in the chain) are

$$\begin{aligned}
\frac{E}{L} &\equiv e_0 = \int_{-B}^B dk k^2 \rho(k) + 2 \int_{-Q}^Q d\lambda [\lambda^2 - (c^2/4)]\sigma(\lambda) \\
&- \mu \frac{N}{L} - H \frac{M_z}{L} - D \frac{\mathcal{L}}{L}, \\
\frac{N}{L} &= \int_{-B}^B dk \rho(k) + 2 \int_{-Q}^Q d\lambda \sigma(\lambda), \\
\frac{M_z}{L} &= \frac{1}{2} \int_{-B}^B dk \rho(k), \\
\frac{\mathcal{L}}{L} &= \int_{-B}^B dk \rho(k) + 2 \int_{-Q}^Q d\lambda \sigma(\lambda) \\
&- 2 \int_{-A_1}^{A_1} d\xi \phi_1(\xi) - 4 \int_{-A_2}^{A_2} d\xi \phi_2(\xi). \quad (\text{B7})
\end{aligned}$$

-
- [1] P. G. de Gennes, *Liquid Crystals* (Clarendon, Oxford, 1974).
- [2] L. D. Landau and E. M. Lifshitz, *Statistical Physics* (Elsevier, Amsterdam, 1980).
- [3] M. P. Kolodyazhnaya, K. R. Zhekov, I. V. Bilych, G. A. Zvyagina, and A. A. Zvyagin, *Fiz. Nizk. Temp.* **43**, 1600 (2017) [*Low Temp. Phys.* **43**, 1276 (2017)].
- [4] R. Okazaki, T. Shibauchi, H. J. Shi, Y. Haga, T. D. Matsuda, E. Yamamoto, Y. Onuki, H. Ikeda, and Y. Matsuda, *Science* **331**, 439 (2011).
- [5] R. Fernandes, A. Chubukov, and J. Schmalian, *Nat. Phys.* **10**, 97 (2014).
- [6] S. Kasahara, H. J. Shi, K. Hashimoto, S. Tonegawa, Y. Mizukami, T. Shibauchi, K. Sugimoto, T. Fukuda, T. Terashima, A. H. Nevidomskyy, and Y. Matsuda, *Nature (London)* **486**, 382 (2012).
- [7] X. Lu, J. Park, R. Zhang, H. Luo, A. H. Nevidomskyy, Q. Si, and P. Dai, *Science* **345**, 657 (2014).
- [8] A. E. Böhrner and A. Kreisel, *J. Phys.: Condens. Matter* **30**, 023001 (2018).
- [9] R. M. Fernandes, A. I. Coldea, H. Ding, I. R. Fisher, P. J. Hirschfeld, and G. Kotliar, *Nature (London)* **601**, 35 (2022).
- [10] S. Acharya, D. Pashov, F. Jamet, and M. van Schilfhaarde, *Symmetry* **13**, 169 (2021).
- [11] K. Haule and G. Kotliar, *New J. Phys.* **11**, 025021 (2009).
- [12] Z. P. Yin, K. Haule, and G. Kotliar, *Nat. Mater.* **10**, 932 (2011).
- [13] P. O. Sprau, A. Kostin, A. Kreisel, A. E. Böhrner, V. Taufour, P. C. Canfield, S. Mukherjee, P. J. Hirschfeld, B. M. Andersen, and J. C. S. Davis, *Science* **357**, 75 (2017).
- [14] M. Yi, Z. Liu, Y. Zhang, R. Yu, J. Zhu, J. Lee, R. Moore, F. Schmitt, W. Li, S. Riggs, J.-H. Chu, B. Lv, J. Hu, M. Hashimoto, S.-K. Mo, Z. Hussain, Z. Mao, C.-W. Chu, I. Fisher, Q. Si *et al.*, *Nat. Commun.* **6**, 7777 (2015).
- [15] T. M. McQueen, A. J. Williams, P. W. Stephens, J. Tao, Y. Zhu, V. Ksenofontov, F. Casper, C. Felser, and R. J. Cava, *Phys. Rev. Lett.* **103**, 057002 (2009).
- [16] Q. Si and E. Abrahams, *Phys. Rev. Lett.* **101**, 076401 (2008).
- [17] R. M. Fernandes and A. V. Chubukov, *Rep. Prog. Phys.* **80**, 014503 (2017).
- [18] O. Vafek and A. V. Chubukov, *Phys. Rev. Lett.* **118**, 087003 (2017).
- [19] P. Coleman, Y. Komijani, and E. J. König, *Phys. Rev. Lett.* **125**, 077001 (2020).
- [20] A. A. Zvyagin, *Finite Size Effects in Correlated Electron Models: Exact Results* (Imperial College Press, London, 2005).
- [21] N. D. Mermin and H. Wagner, *Phys. Rev. Lett.* **17**, 1133 (1966).
- [22] E. Barouch and B. M. McCoy, *Phys. Rev. A* **3**, 786 (1971).
- [23] P. Pfeuty, *Ann. Phys. (Amsterdam)* **57**, 79 (1970).
- [24] A. Georges, L. de Medici, and J. Mravlje, *Annu. Rev. Condens. Matter Phys.* **4**, 137 (2013).
- [25] A. A. Zvyagin and P. Schlottmann, *Phys. Rev. B* **60**, 6292 (1999).
- [26] P. P. Kulish and E. K. Sklyanin, *Phys. Lett. A* **84**, 349 (1981).
- [27] C. N. Yang, *Phys. Rev. Lett.* **19**, 1312 (1967).
- [28] M. Gaudin, *Phys. Lett. A* **24**, 55 (1967).
- [29] P. Schlottmann, *Phys. Rev. B* **49**, 6132 (1994).
- [30] A. A. Zvyagin and P. Schlottmann, *Nucl. Phys. B* **565**, 555 (2000).
- [31] E. Walter, K. M. Stadler, S. S. B. Lee, Y. Wang, G. Kotliar, A. Weichselbaum, and J. von Delft, *Phys. Rev. X* **10**, 031052 (2020).
- [32] V. Drouin-Touchette, E. J. König, Y. Komijani, and P. Coleman, *Phys. Rev. Res.* **4**, L042011 (2022).
- [33] W. A. Harrison, *Solid State Theory* (McGraw-Hill, New York, 1970).

- [34] J. M. Ziman, *Principles of the Theory of Solids* (Cambridge University Press, Cambridge, 1972).
- [35] N. W. Ashcroft and N. D. Mermin, *Solid State Physics* (Holt, Rinehart and Wilson, New York, 1976).
- [36] W. Heitler, *Z. Phys.* **46**, 47 (1927); **47**, 835 (1928); **51**, 805 (1928).
- [37] F. London, *Z. Phys.* **46**, 455 (1928); **50**, 24 (1928).
- [38] J. Hubbard, *Proc. R. Soc. A* **276**, 238 (1963); **277**, 237 (1964); **281**, 401 (1964); **285**, 542 (1965); **296**, 82 (1967); **296**, 100 (1967).
- [39] E. H. Lieb and F. Y. Wu, *Phys. Rev. Lett.* **20**, 1445 (1968).
- [40] F. H. L. Essler, H. Frahm, F. Göhmann, A. Klümper, and V. E. Korepin, *The One-Dimensional Hubbard Model* (Cambridge University Press, Cambridge, 2005).